

Fabrication of halogen-free ammonium phosphate with two components via a simple method and its flame retardancy in polypropylene composites

Zaihang Zheng^{1,2} · Yan Liu² · Long Zhang¹ · Boya Dai¹ · Xudong Yang¹ · Hongyan Wang³

Received: 28 March 2016 / Accepted: 8 August 2016 / Published online: 30 August 2016
© Akadémiai Kiadó, Budapest, Hungary 2016

Abstract In this paper, a halogen-free flame retardant with two different functional components was prepared via a simple method. The novelty of this work is the combination of acid source and char-forming agent in one compound simultaneously. And the advantage of this method lies in effectively avoiding the mixture of several components for composites during thermal processing and improving the flame retardancy of polymers. Besides, the chemical structure of modified ammonium phosphate (MAPP) was confirmed by Fourier transform infrared spectra (FTIR) and X-ray diffraction spectra (XRD), respectively. The results indicate that thermal decomposition process of APP after modification is obviously changed. When polypropylene (PP) is composited with 30 phr MAPP, the limiting oxygen index value can reach 28.5 % and pass vertical burning tests (UL-94) V-1 rating. Simultaneously, thermal gravimetric analysis demonstrates that the introduction of diethanolamine can improve the char-forming rate and char residue of PP/APP composites. Except that, the thermal pyrolysis of MAPP detected by FTIR spectra deduces that the char-forming process

happens at 350–400 °C. The analysis on char residue after combustion indicates that the cross-linking bonds of P–O–C groups appear. At last, a potential condensed mechanism was primarily proposed.

Keywords Ammonium phosphate · Modification · Mono-component · Flame retardancy · Polypropylene

Introduction

Due to the advantages in mechanical properties, thermal performance, chemical resistance properties, electrical properties and processing behavior, polypropylene (PP) materials are widely applied in lots of fields, such as automotive industry, consumer goods, containers, nonwoven fabrics and electric industry [1–4]. However, the flammability of PP materials greatly restrains its further application [5–7]. In this condition, the development on the flame retardants to solve this problem becomes an urgent issue. Recently, halogen-free and intumescent flame retardants (IFR) were gradually exploited by many researchers [8–10]. Camino et al. [11–15] had performed a great deal of experiments on several IFR systems. During these investigation, the most representative IFR system is a combination of ammonium polyphosphate (APP), pentaerythritol (PER) and melamine (MEL). Here, they act as acid source, carbon agent and gas source in IFR system, respectively. Except that, Camino et al. [16] had deeply studied the expansion behavior of APP/PER by adopting pentaerythritol diphosphate (PEDP) as a model compound and proposed the main expansion mechanism of this system [17–19].

Unfortunately, the flame retardant efficiency for APP/PER/MEL system is not high enough. When this system is

Electronic supplementary material The online version of this article (doi:10.1007/s10973-016-5779-x) contains supplementary material, which is available to authorized users.

✉ Zaihang Zheng
zhengzaihang@ccut.edu.cn

¹ School of Chemical Engineering, Changchun University of Technology, Changchun 130012, People's Republic of China

² Key Laboratory of Bionic Engineering (Ministry of Education), Jilin University, Changchun 130022, People's Republic of China

³ College of Chemistry, Jilin University, Changchun 130012, People's Republic of China

applied in the actual life, it usually needs a large amount of flame retardants to achieve the ideal flame retardancy. And the ternary IFR system may affect the processing procedure in preparing polymer composites. For this purpose, scientists have exploited many practical methods to solve these disadvantages. Nowadays, the focus has been concentrated on preparing the multiple flame retardants in improving the efficiency. Especially, the combination of acid resource and char-forming agent in mono-component compound is the main trend in the field of flame retardants. This idea can improve the flame retardant efficiency of IFR and simplify the processing procedure of composites simultaneously.

In this paper, we have prepared modified ammonium polyphosphate (MAPP) by the introduction of diethanolamine onto the side chains of ammonium polyphosphate. The products can act as acid source and char-forming agent in IFR system simultaneously. The chemical structure of MAPP was detected by Fourier transform infrared spectra (FTIR) and X-ray diffraction spectra (XRD), respectively. Except that, thermal gravimetric analysis (TG) systematically investigates the thermal stability and char residue of PP composites. Furthermore, the thermal pyrolysis process of MAPP was monitored by FTIR spectra in order to investigate the changes in chemical structure during different temperature. And the char-forming temperature can roughly be achieved from the changes in FTIR spectra of char residue. Finally, the possible flame retardant mechanism of MAPP in PP matrix was proposed by analyzing the char residue in detail.

Experimental

Materials

Polypropylene (PP, melt flow index, $2.5 \text{ g } 10 \text{ min}^{-1}$) was provided by Yangzi Petroleum Chemical Company. Ammonium polyphosphate (APP) (phase II, the degree of polymerization >1500 ; density, 1.88 g cm^{-3}) brought from Qingdao Haida Chemical Co., Ltd. was under $80 \text{ }^\circ\text{C}$ vacuum drying before using. Anhydrous alcohol and diethanolamine were obtained from Aldrich. The deionized water used in this experiment was distilled followed by deionization.

Preparation of ammonium phosphate with two components

The experiments were carried out under nitrogen atmosphere in a 1000-mL four-neck flask equipped with reflux condenser, mechanical stirrer and dropping funnel were heated in the water bath. At first, 100 g APP and 54 g diethanolamine were added into four-neck flask. At the same time, 350 mL deionized water and 40 mL anhydrous

alcohol were poured into the system. Then, the system was sonicated for 15 min in order to promote the homogeneous dispersion of APP in mixture solvent. The mixture was heated to $90 \text{ }^\circ\text{C}$ and kept for 4 h. After that, the system was cooled down to room temperature and filtrated under vacuum. The products were washed with deionized water and anhydrous alcohol several times and dried at $70 \text{ }^\circ\text{C}$ for 24 h (Scheme 1).

Preparation of flame-retarded PP composites

PP and flame retardants were melt-mixed in a twin-screw extruder. Temperatures along the barrel were 110, 190, 190, 190, 190 and $185 \text{ }^\circ\text{C}$ in the section of heating module in sequence. When the temperature reaches the default value, the feeding process was started. The screw rotating and feeding speeds were set as 30 rpm and 12 rpm, respectively. After the mixing process continues for 15 min, the composites were injected and cut to particles. Subsequently, the particles were hot-pressed at $190 \text{ }^\circ\text{C}$ under 10 MPa for 15 min into sheets of suitable thickness for measurement. The sample formulations are listed in Table 1.

Characterization

Fourier transform infrared spectra (FTIR)

The infrared spectra of the samples were recorded with an FTIR SHIMADZU spectrometer at a resolution of 2 cm^{-1} . FTIR spectra of the samples were obtained between 4000 and 400 cm^{-1} on a KBr powder with an FTIR spectrometer.

X-ray diffraction spectra (XRD)

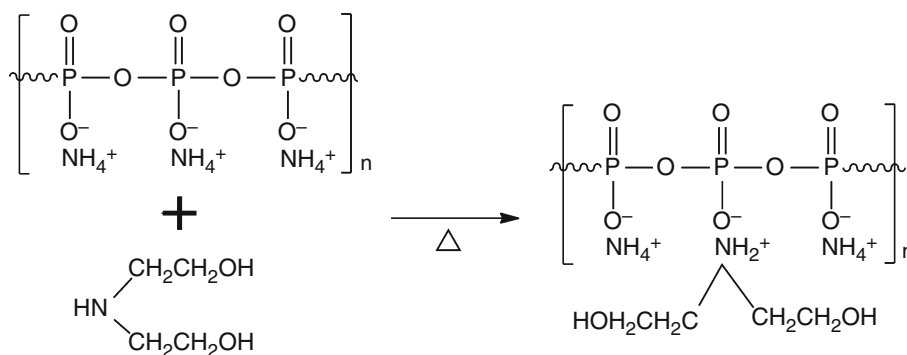
X-ray diffraction spectra of samples were detected by a SHIMADZU X-ray diffraction spectra instrument. The scanning speed is $2 \text{ }^\circ \text{ min}^{-1}$ from 10° to 60° .

Elemental analysis

The carbon, hydrogen, nitrogen and oxygen contents of APP and MAPP were determined with a Perkin-Elmer 240 analyzer. The analyses were performed with 1 mg of sample ground and sieved to $<0.2 \text{ mm}$. The results were quoted as the mean of values from four determinations. In all cases, the experimental error was $<0.5 \%$ of the absolute value.

Scanning electron microscope (SEM)

The morphology of char residue after combustion was investigated by SHIMADZU S5X-550 scanning electron microscope. The specimens were sputter-coated with a conductive gold layer. The accelerated voltage was 20 kV.

Scheme 1 Preparation and structure of MAPP**Table 1** Results of LOI and UL-94 tests for PP composites

Sample	PP/phr	APP/phr	MAPP/phr	LOI/%		UL-94	
				Untreated	Treated	Untreated	Treated
PP	100	0	0	17.0	17.0	No rating	No rating
PP/APP	100	30	0	20.0	17.5	No rating	No rating
PP/MAPP	100	0	30	28.5	18.0	V-1	No rating

Thermogravimetric analysis (TG)

All of samples were dried overnight before measurement. The TG curves were recorded on a Pyris Diamond TG/DTA (Perkin-Elmer) under 50 mL min⁻¹ nitrogen flow ratio from 50 to 850 °C at a heating rate of 10 °C min⁻¹. The sample mass was 5–10 mg.

Limiting oxygen index (LOI)

The LOI tests were carried out by using an XZT-100A oxygen index test instrument (Chengde Jiande test instrument Co., Ltd., China) based on the standard LOI test, ASTM D 2863-97. The dimensions of specimens were 127 × 10 × 10 mm³. The test method is generally reproducible to an accuracy of ±0.1 %.

Vertical burning test (UL-94)

The vertical burning test was carried out on a CFZ-2-type instrument (Jiangning Analysis Instrument Company, China) according to the UL-94 test standard. The specimens used were of dimensions 130 × 13 × 3 mm³.

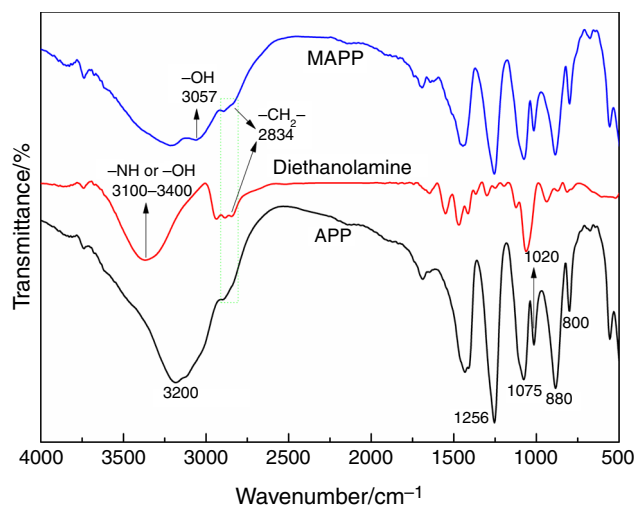
X-ray photoelectron spectroscopy (XPS) spectra

The XPS spectra of char residue were recorded with a VG ESCALABMK II spectrometer using Al ka excitation radiation ($h\nu = 1253.6$ eV).

Results and discussion

FTIR spectra of APP and MAPP

FTIR spectra of APP, diethanolamine and MAPP are shown in Fig. 1. The typical absorption peaks of APP contain 3200 (–NH), 1256 (P=O), 1075 (P–O symmetric vibration), 1020 (symmetric vibration of PO₂ and PO₃), 880 (P–O asymmetric vibration) and 800 (P–O–P) cm⁻¹ [20, 21]. For diethanolamine, the absorption peaks of –NH or –OH groups and –CH₂– groups appear at 3100–3400 and 2834 cm⁻¹, respectively. After modification, the new

**Fig. 1** FTIR spectra of APP, diethanolamine and MAPP

peaks at 3057 and 2834 cm^{-1} appear in the FTIR spectra of MAPP. Obviously, these peaks are assigned to $-\text{OH}$ groups and $-\text{CH}_2-$ groups from diethanolamine even if some shift occurs for $-\text{OH}$ groups. These facts demonstrate the diethanolamine has been grafted onto the side chain of APP. Besides, the main characteristic absorption of APP nearly keeps unchanged, illustrating that the chemical main chain of APP is not broken.

XRD spectra of APP and MAPP

The chemical structure of APP and MAPP was also investigated by XRD spectra, as shown in Fig. 2. It can be seen that the XRD spectra between APP and MAPP are very similar. This fact indicates that the whole lattice structure of APP is nearly not influenced after modification.

Elemental analysis of APP and MAPP

Table 2 presents the results of elemental analysis of APP and MAPP. Compared with APP, the element content of MAPP obviously changes after modification. The content of carbon and hydrogen increases while the content of oxygen and nitrogen decreases. As we know, the element content of carbon and hydrogen is large in the molecular chain of diethanolamine. Thus, it is intuitively observed that the diethanolamine molecules were introduced into the molecular chain of APP. Along with FTIR and XRD spectra, the feasibility for modifying APP is confirmed.

Thermal behavior of APP and MAPP

The thermal behavior of APP and MAPP was investigated by TG, as shown in Fig. 3. Besides, the derivative thermogravimetry (DTG) of TG curves is also investigated in

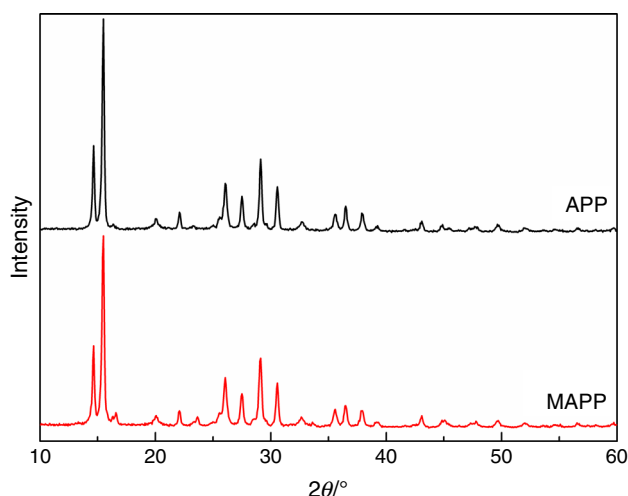


Fig. 2 XRD spectra of APP and MAPP

Fig. 3b. It can be observed that the thermal degradation curve of APP is mainly composed of two steps. In first step, APP presents an obvious decomposition at 300–530 $^{\circ}\text{C}$ with about 20 mass% mass loss, which is attributed to the release of the volatile products (NH_3 and H_2O) and the formation of a highly cross-linked polyphosphoric acids (PPA) [22–24]. With the temperature increasing, the further decomposition of PPA leads to the formation of P_2O_5 and P_4O_{10} in the second step, which leaves 14 mass% residual mass. For MAPP, the thermal decomposition temperature evidently decreases due to the introduction of diethanolamine onto APP chains. Moreover, the temperature at maximum decomposition rate of MAPP is about 90 $^{\circ}\text{C}$ higher than that of APP. This is mostly attributed to the formation of char residue with high thermal stability. Moreover, the char residue of MAPP is much more than that of APP when the temperature is 600–800 $^{\circ}\text{C}$. This fact is ascribed to the incorporation of diethanolamine onto APP molecular chains. The thermal interaction between APP and diethanolamine can produce more char residue with high thermal stability. When the temperature is above 800 $^{\circ}\text{C}$, the char residue is destroyed and further starts to decompose. It leads to that the char residue of MAPP is the same as the char residue of APP.

Flame retardancy

Generally, limiting oxygen index (LOI) and vertical burning (UL-94) tests are the most basic methods in assessing the flame retardancy of materials. As shown in Table 1, LOI value of pure PP is 17.0 % indicate the flammability of PP. Besides, PP cannot pass the UL-94 tests because of severe melt dripping phenomenon. When PP is composited with 30 phr APP, the LOI value of PP/APP reaches 20.0 %. Due to lack of char-forming agent, APP is not very effective in flame-retarding PP materials when used alone. In this condition, PP/APP still cannot achieve the ratings in UL-94 tests. For PP/MAPP, LOI value further raises to 28.5 % and obtains a V-1 rating in UL-94 tests. It illustrates that the flame retardant properties of PP/APP composites are greatly improved by the incorporation of char agent into the system.

Except that, we have investigated the flame retardancy of PP composites by water treatment. The water treatment process is carried out by soaking PP composites in 60 $^{\circ}\text{C}$

Table 2 Elemental analysis of APP and MAPP

Sample	C/%	H/%	O/%	N/%
APP	–	4.13	49.47	14.45
MAPP	16.03	6.36	42.82	4.68

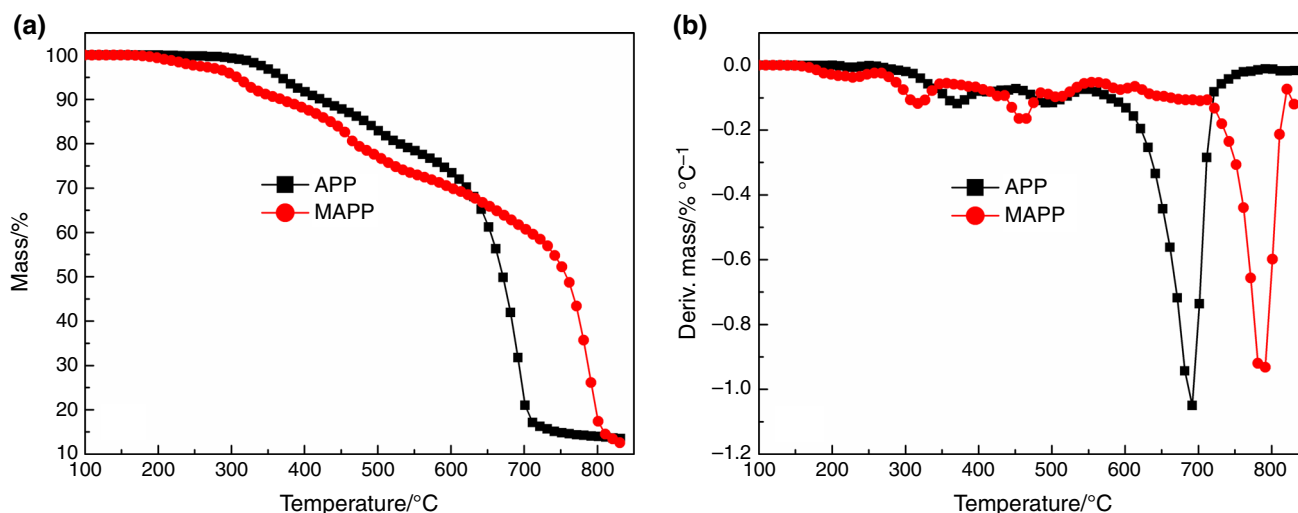


Fig. 3 Thermal behavior of APP and MAPP, **a** TG curves, **b** DTG curves

water for 24 h. Then, the flame retardancy of PP composites after hot water treatment was measured after the samples were taken out and dried in room temperature. It can be obviously seen that the flame retardant properties greatly decrease for both APP and MAPP. For PP/APP, the decrease in flame retardancy is ascribed to the weak water resistance of APP with the hydrophilic groups. After the introduction of diethanolamine onto APP, the water sensitivity further increases due to the structure of $-OH$ and $-NH$ groups on MAPP. Thus, when PP/MAPP is exposed to water, the MAPP particles will completely emigrate from composites into water. In this condition, the flame retardancy of PP/MAPP nearly disappears that is equivalent to the transition from PP/MAPP to pure PP. In our future paper, we will focus on solving this defect of MAPP by surface modification.

Thermogravimetric analysis of PP composites

The thermal degradation of PP, PP/APP and PP/MAPP in nitrogen was investigated, as shown in Fig. 4. Besides, the derivative thermogravimetry (DTG) of TG curves was also investigated, as shown in Fig. 4b. The detailed data are listed in Table 3, which includes the temperature at 5 % mass loss (T_{on}), the maximum mass loss temperature (T_{max}) and the residual mass at 500, 600 and 700 °C, respectively. Obviously, the initial decomposition temperature of PP is 300 °C. When the temperature is above 450 °C, PP completely degrades that demonstrates its poor char-forming ability. Furthermore, this is the main reason for the flammability of PP materials. As previously reported [25], both T_{on} and T_{max} values of PP/APP are higher than that of PP. This is ascribed that the thermal decomposition temperature of APP is higher than PP itself. Due to the presence of APP, the char residue of PP/APP is also improved. After chemical modification of

APP, the T_{max} value further increases, indicating that the thermal stability of PP composites is enhanced. Except that, the char residue of PP/MAPP is much higher than PP/APP at high temperature. The char residue for PP/MAPP at 500, 600 and 700 °C is 15.53, 13.15 and 10.89 %, respectively. This char residue with high thermal stability is feasible to improve the flame retardancy of PP materials. As shown in Fig. 4 and Table 3, the R_{max} value of PP/MAPP is larger than that of PP and PP/APP. The large R_{max} value is ascribed that the char-forming rate of PP/MAPP during thermal flow is much faster than that of PP and PP/APP. In this paper, the inflection point is the point in the fastest slope change of TG curves when the main thermal decomposition is near finishing. At this point, the char-forming process is close to complete. (The thermal degradation rate of char residue obviously slows down). And it is approximately equivalent to the “0” value in Y axis of DTG curves after the peak (R_{max}). The temperature at inflection point has been labeled in Fig. 4a. Compared with PP and PP/APP, it can be obviously found that the degradation temperature region from T_{on} to inflection point of PP/MAPP is much narrower than PP/APP. In another word, the temperature difference of PP/MAPP between initial decomposition and the main decomposition end for PP composites is less than PP/APP. In this condition, it is considered that the char-forming rate of PP/MAPP is faster than that of PP/APP. In this condition, R_{max} value of PP/MAPP was larger than that of PP and PP/APP. Except that, the large R_{max} value cannot affect the content of char residue for PP/MAPP in contrast with that of PP and PP/APP, as shown in Fig. 4 and Table 3.

Thermal oxidative process analysis of MAPP

In order to further study the char-forming process for MAPP during the thermal degradation, the char residue

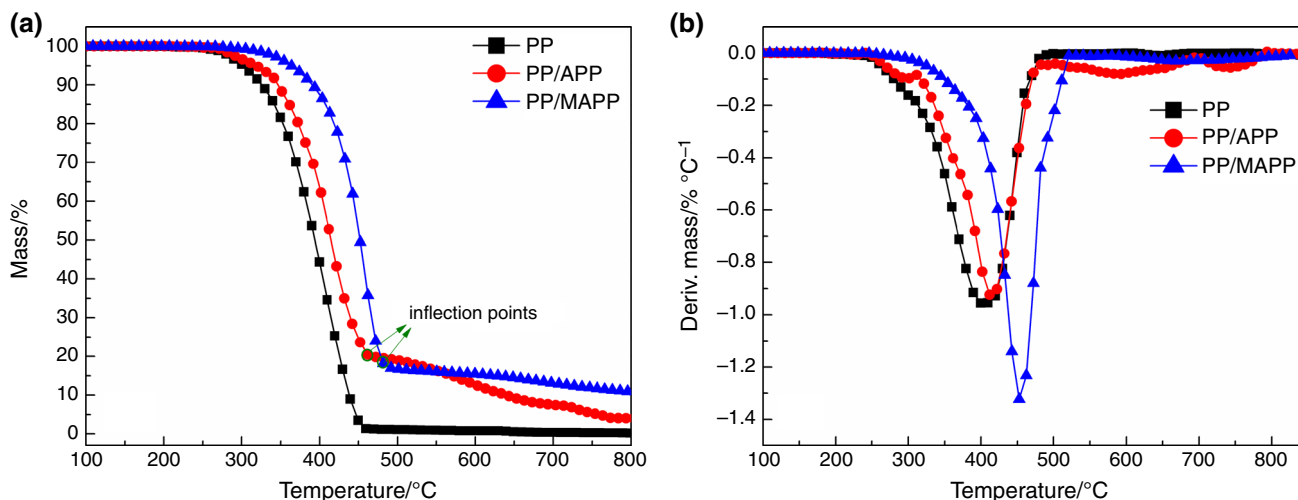


Fig. 4 Thermal behavior of PP composites, **a** TG curves, **b** DTG curves

Table 3 Data for the thermal decomposition of PP composites

Sample	$T_{on}/^{\circ}\text{C}$	$T_{max}/^{\circ}\text{C}$	Char residue/mass%			$R_{max}/\% \text{ } ^{\circ}\text{C}^{-1}$
			500 °C	600 °C	700 °C	
PP	300.1	406.8	0	0	0	-0.964
PP/APP	318.6	414.4	19.13	12.54	7.55	-0.924
PP/MAPP	364.5	451.3	15.53	13.15	10.89	-1.324

T_{on} , the temperature at 5 % mass loss; T_{max} , the temperature at maximum mass loss rate; R_{max} , maximum decomposition rate

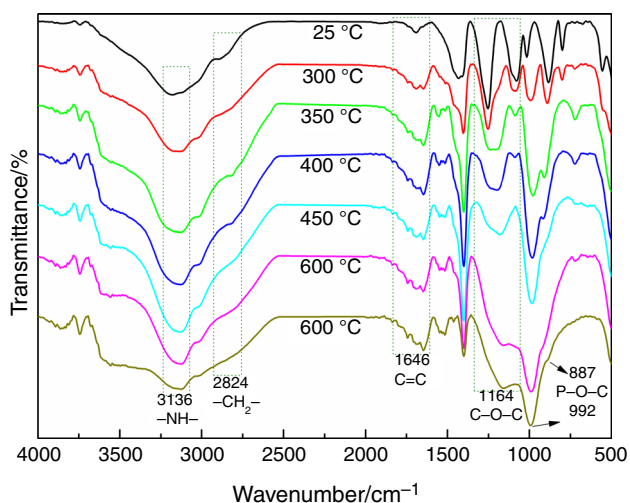


Fig. 5 Analysis on thermal pyrolysis process of MAPP

obtained at different thermal pyrolysis temperature was characterized by FTIR spectra. MAPP was heated in $10 \text{ } ^{\circ}\text{C min}^{-1}$ heating rate in thermal gravimetric analyzer in air atmosphere [26]. The residues were obtained by heating MAPP to 300, 350, 400, 450, 500 and 600 °C in air and

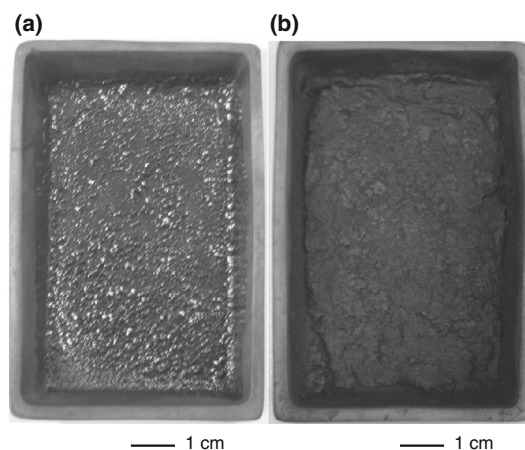


Fig. 6 Optical photos of char residue for PP composites after combustion, **a** PP/APP, **b** PP/MAPP

maintained 10 min at every temperature, respectively. The detailed FTIR curves of these residues are shown in Fig. 5. It can be obviously seen that the FTIR spectra of MAPP at 300 °C are quite different from that at 25 °C. Here, the characteristic absorption of -NH groups is 3136 cm^{-1} . The

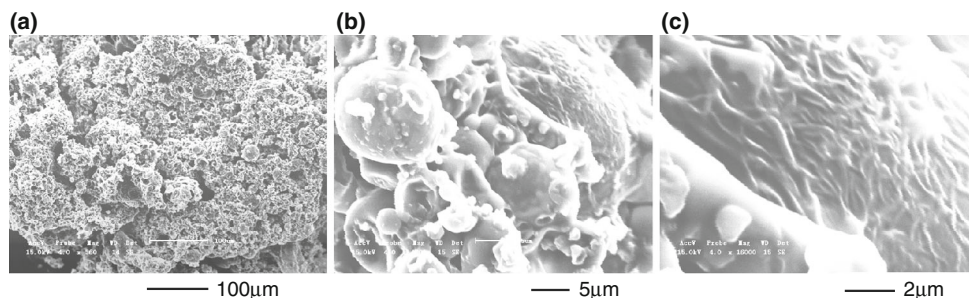


Fig. 7 SEM photos of char residue for PP/MAPP after combustion at different magnification, **a** 100 μm , **b** 5 μm , **c** 2 μm

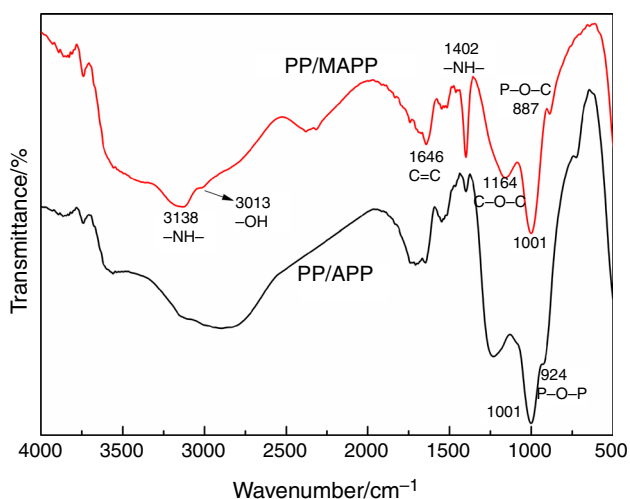


Fig. 8 FTIR spectra of char residue for PP/APP and PP/MAPP after combustion

new peak at 1646 cm^{-1} is originated from the appearance of $\text{C}=\text{C}$ groups. This indicates that the thermal decomposition of MAPP occurs. When the temperature raises to $350\text{ }^{\circ}\text{C}$, the peak at 1258 cm^{-1} occurs the cleavage into two peaks. The peak at 1164 cm^{-1} is ascribed to the absorption of $\text{C}-\text{O}-\text{C}$ groups. Except that, the characterized absorption at 2824 cm^{-1} that represents $-\text{CH}_2-$ groups gradually disappears with the temperature. This is caused by the thermal decomposition of diethanolamine in MAPP. Furthermore, the new peaks appear at 992 and 887 cm^{-1} , which is originated from the $\text{P}-\text{O}$ bonds on the $\text{P}-\text{O}-\text{C}$ groups. This demonstrates that the cross-linking reaction of MAPP proceeds to generate the char residue. Therefore, it can be obtained that the main char-forming temperature of MAPP is $350\text{--}400\text{ }^{\circ}\text{C}$. This can further explain the increase in the thermal stability for PP/MAPP.

The analysis of PP composites after combustion

To investigate the flame retardant mechanism of MAPP in PP matrix, the char residue of PP/MAPP after combustion

was systematically researched by optical photos, SEM, FTIR spectra and XPS spectra, respectively. Optical photos demonstrate that the char residue of PP/APP is inconsecutive due to the lack of char agent in Fig. 6a. As for PP/MAPP, the char-forming content obviously increases and the char residue presents expandable and dense surface due to the introduction of char agent into APP system. In view of microscopic morphology, the “bubble-like” intumescent structure of char residue was obviously observed, as shown in Fig. 7a, b. Moreover, the surface of char layer is quite compact and rough. This is mainly ascribed to the chemical reaction between char-forming section and acid source section from MAPP. This can restrain both mass and heat transfer between gas phase and condensed phase and protect the underlying material from further decomposition. Furthermore, it can improve the flame retardancy of PP materials via condensed mechanism. FTIR spectra of char residue are shown in Fig. 8. As for PP/APP, the peaks at 1001 and 924 cm^{-1} indicate the char residue of PP/APP is composed of phosphorus oxide. Compared with PP/APP, the peaks at 3138 and 1402 cm^{-1} for PP/MAPP are assigned to the absorption of $-\text{NH}-$ groups. This may be originated from the formation of nitrogen-containing heterocyclic structure [27]. In addition, the characterization absorption at 3013 , 1646 and 1164 cm^{-1} is ascribed to $-\text{OH}$, $\text{C}=\text{C}$ and $\text{C}-\text{O}-\text{C}$ groups, respectively. All of them are generated from the thermal decomposition of MAPP. Except that, the $\text{P}-\text{O}$ bonds on $\text{P}-\text{O}-\text{C}$ groups appear at 1001 and 887 cm^{-1} that confirms the esterifiable cross-linking reaction between MAPP particles [28, 29]. It can promote the formation of char layer and further improve the flame retardancy of PP.

Besides, the surface composition of char residue from PP/MAPP after combustion was systematically analyzed by XPS spectra. The char residue spectra of C_{1s} , O_{1s} , N_{1s} and P_{2p} are shown in Fig. 9. Besides, the detailed assignment of these peaks is recorded in Table 4. In C_{1s} spectra, the peaks at 284.8 and 286.3 eV are assigned to $\text{C}-\text{C}$ bonds in aliphatic and aromatic structures and $\text{C}-\text{O}$ bonds in the $\text{P}-\text{O}-\text{C}$ groups in ether and phosphate or $\text{C}-\text{O}-\text{C}$ bond in

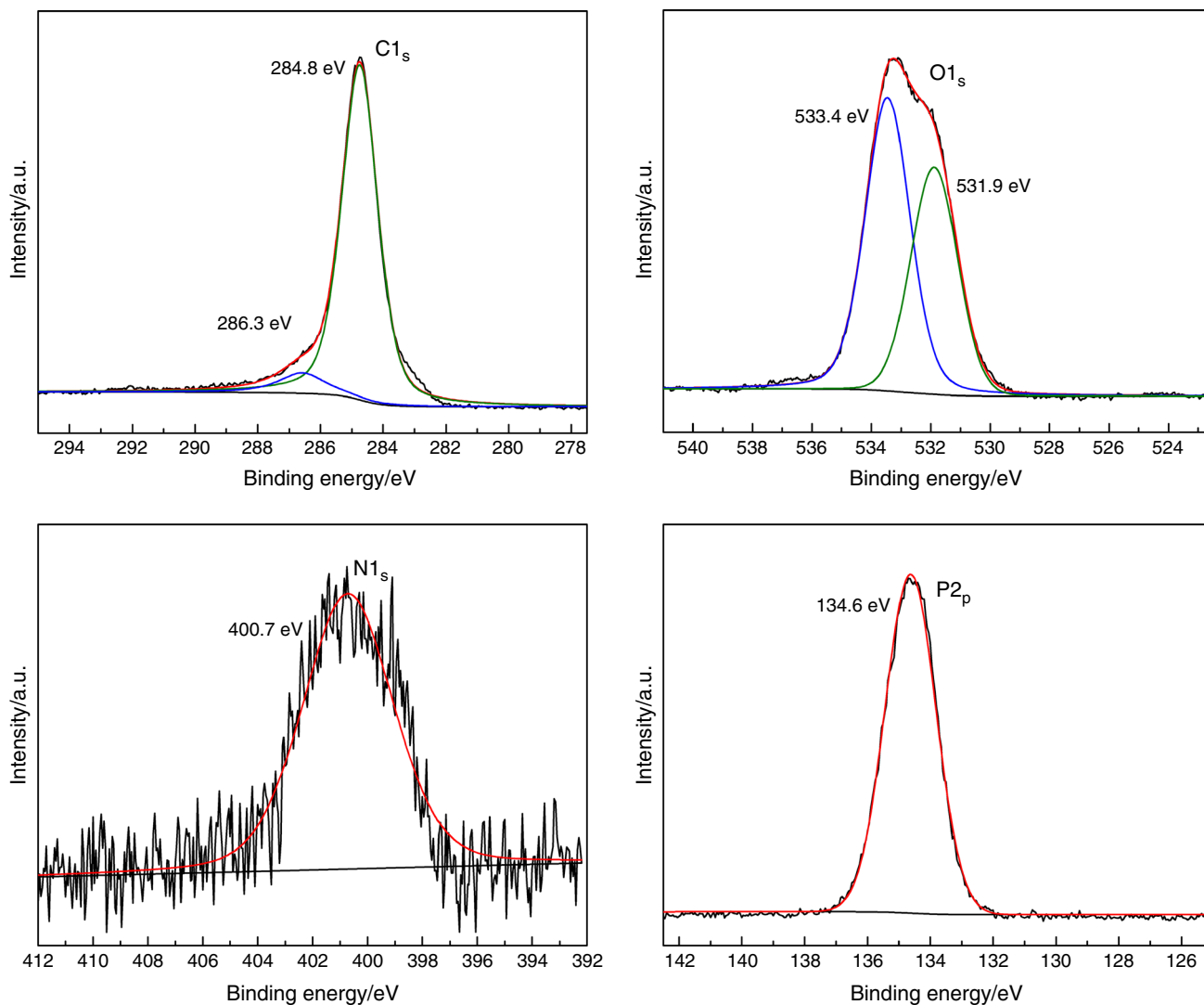


Fig. 9 XPS spectra of char residue for PP/MAPP after combustion

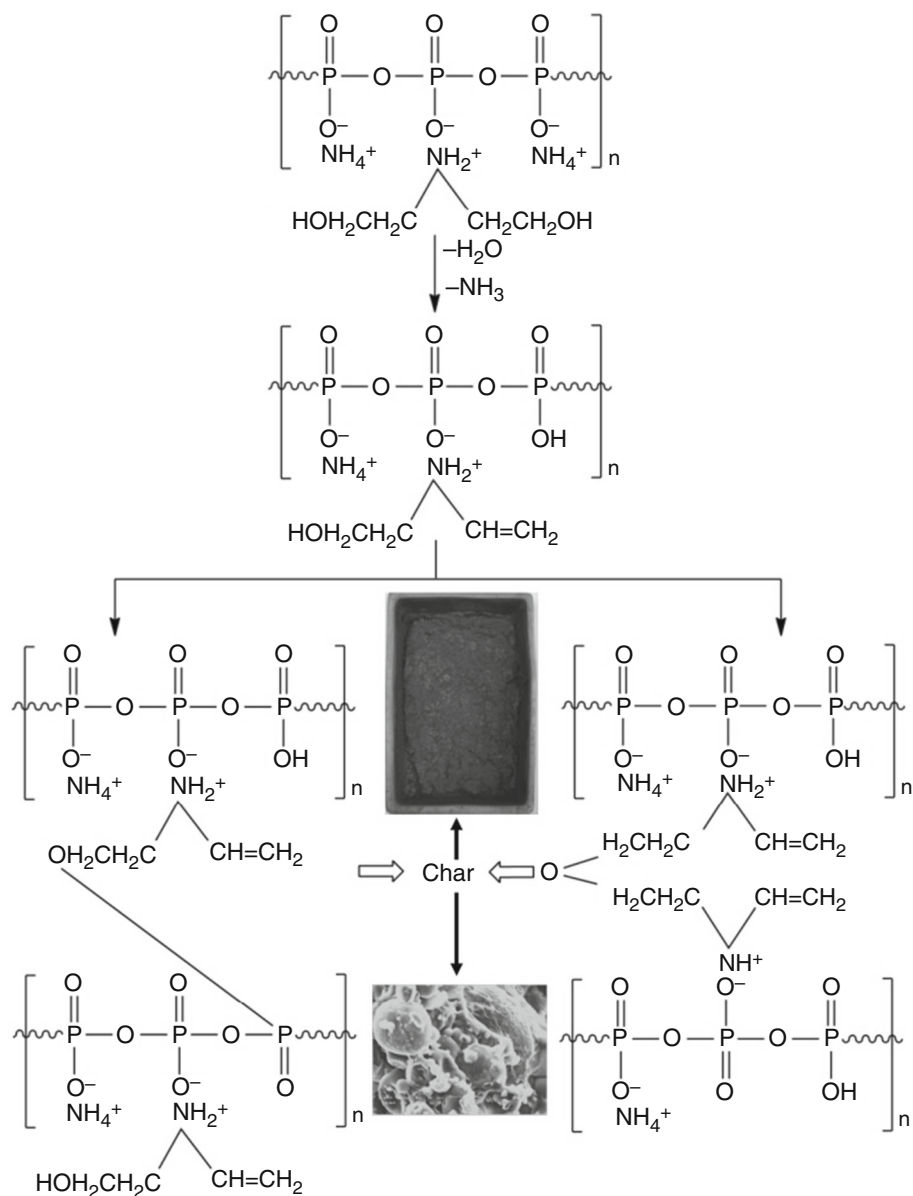
Table 4 Functional groups identification of char residue from PP/MAPP

Element	Element content/%	Binding energy/eV	Identification
C _{1s}	62.72	284.8	C–C
		286.3	C–O or P–O–C
O _{1s}	18.62	531.9	–O–
		533.4	C=O
N _{1s}	2.85	400.7	Heterocyclic ring
P _{2p}	15.82	134.6	P–O–C

ester and other carbonyl compounds. This fact is well consistent with FTIR spectra above. XPS spectra of O_{1s} at 531.9 and 533.4 eV are attributed to the –O– and =O– bonds in C–O–C, P–O–C and C=O groups [10]. This also confirms the results of the C_{1s} peak. And N_{1s} spectra at

400.7 eV are generated from the nitrogen-containing heterocyclic structure [30, 31]. But the content of N element in the char residue is so tiny that it cannot play the main role in flame-retarding PP. As for P_{2p} spectra, the band at 134.6 eV demonstrates the cross-linking bands (C–

Scheme 2 Potential char-forming process of MAPP in PP composites



O–P) are formed by esterification of MAPP during thermal decomposition of PP composites [32, 33]. These results can explain the char-forming process of PP/MAPP and the main flame retardant mechanism.

Potential char-forming process of MAPP in PP composites

Based on these facts, the potential char-forming process of MAPP in PP composites was proposed, as shown in Scheme 2. First, the inert gases release from APP during thermal degradation at 300–500 °C. At the same time, the decomposition of APP produces polyphosphoric acid (PPA). After that, the further reaction of MAPP was

divided into two procedures. In one hand, the thermal esterification reaction occurs between hydroxyl groups and phosphoric acid groups from APP that generates the P–O–C cross-linking groups. The introduction of diethanolamine makes the APP particles possess the acid source and char-forming agent simultaneously; on the other hand, the dehydration reaction between MAPP forms the ether groups. These facts were confirmed by FTIR and XPS spectra, as presented in Figs. 8 and 9. This residue collectively constructs the char layer on the surface of materials. Besides, the inert gases from the thermal degradation of APP can promote this char-forming process to produce the dense, swell and compact surface. This char layer can greatly protect the underlying substrate from further

thermal decomposition. Furthermore, this process can improve the flame retardant properties of PP materials via the condensed process.

Conclusions

In this paper, the char-forming agent (diethanolamine) was introduced into the molecular chains of acid source (APP) that fabricates the “two components in one” pattern flame retardant (MAPP). FTIR and XRD spectra confirm the chemical structure of MAPP. The results demonstrate that when composited with 30 phr MAPP, PP composites can reach 28.5 % LOI value and UL-94 V-1 rating. Moreover, thermal gravimetric analysis indicates that the introduction of MAPP can improve the thermal stability and char residue of PP composites. FTIR spectra on thermal pyrolysis indicate that the char-forming temperature of MAPP focuses at 350–400 °C. Except that, the char residue of PP/MAPP after combustion was systematically investigated by optical photos, SEM, FTIR and XPS spectra. The fact illustrates that the dense and intumescent char layer composed of P–O–C groups was generated during combustion. Finally, the potential char-forming process of MAPP in PP is proposed.

References

- Xian JM, He ZQ, Li MQ, Lin ZD, Chen JX, Yang QG, Xiao L, Li W. Preparation and properties of coral/ β -polypropylene bio-composites. *J Therm Anal Calorim.* 2015;122:1005–11.
- Marčin A, Ujhelyiová A, Marčin K, Hricová M. Spinning, mechanical and thermal properties of metallocene polypropylene fibers. *J Therm Anal Calorim.* 2015;1:1–13.
- Papageorgiou DG, Filippousi M, Pavlidou E, Chrissafis K, Tendeloo GV, Bikiriadis D. Effect of clay modification on structure–property relationships and thermal degradation kinetics of β -polypropylene/clay composite materials. *J Therm Anal Calorim.* 2015;122:393–406.
- Alaburdaitė R, Krylova V. Study of thermo-oxidative chemical pre-treatment of isotactic polypropylene. *J Therm Anal Calorim.* 2014;118:1331–8.
- Zheng ZH, Liu SF, Wang BN, Yang T, Cui XJ, Wang HY. Preparation of a novel phosphorus- and nitrogen-containing flame retardant and its synergistic effect in the intumescent flame-retarding polypropylene system. *Polym Compos.* 2015;36:1606–19.
- Chen XL, Song WK, Liu JB, Jiao CM, Qian Y. Synergistic flame-retardant effects between aluminum hypophosphite and expandable graphite in silicone rubber composites. *J Therm Anal Calorim.* 2015;120:1819–26.
- Nie SB, Zhou C, Peng C, Liu L, Zhang C, Dong X, Wang DY. Thermal oxidative degradation kinetics of novel intumescent flame-retardant polypropylene composites. *J Therm Anal Calorim.* 2015;120:1183–91.
- Chen YJ, Guo ZH, Fang ZP. Relationship between the distribution of organo-montmorillonite and the flammability of flame retardant polypropylene. *Polym Eng Sci.* 2012;52:390–8.
- Zheng ZH, Yang T, Wang BN, Qu BB, Wang HY. Microencapsulated melamine phosphate via the sol–gel method and its application in halogen-free and intumescent flame-retarding acrylonitrile-butadiene-styrene copolymer. *Polym Int.* 2015;64:1275–88.
- Liu Y, Zhao J, Deng CL, Chen L, Wang DY, Wang YZ. Flame-retardant effect of sepiolite on an intumescent flame-retardant polypropylene system. *Ind Eng Chem Res.* 2011;50:2047–54.
- Camino G, Costa L, Trossarelli L. Study of the mechanism of intumescence in fire retardant polymers: part I—thermal degradation of ammonium polyphosphate–pentaerythritol mixtures. *Polym Degrad Stabil.* 1984;6:243–52.
- Camino G, Costa L, Trossarelli L. Study of the mechanism of intumescence in fire retardant polymers: part II—mechanism of action in polypropylene–ammonium polyphosphate–pentaerythritol mixtures. *Polym Degrad Stabil.* 1984;7:25–31.
- Camino G, Costa L, Trossarelli L. Study of the mechanism of intumescence in fire retardant polymers: part III—effect of urea on the ammonium polyphosphate–pentaerythritol system. *Polym Degrad Stabil.* 1984;7:221–9.
- Camino G, Costa L, Trossarelli L, Costanzi F, Landoni G. Study of the mechanism of intumescence in fire retardant polymers: part IV—evidence of ester formation in ammonium polyphosphate–pentaerythritol mixtures. *Polym Degrad Stabil.* 1984;8:13–22.
- Camino G, Costa L, Trossarelli L. Study of the mechanism of intumescence in fire retardant polymers: part V—mechanism of formation of gaseous products in the thermal degradation of ammonium polyphosphate. *Polym Degrad Stabil.* 1985;12:203–11.
- Camino G, Costa L, Trossarelli L. Study of the mechanism of intumescence in fire retardant polymers: part VI—mechanism of ester formation in ammonium polyphosphate–pentaerythritol mixtures. *Polym Degrad Stabil.* 1985;13:213–28.
- Gao M, Wu W, Yan Y. Thermal degradation and flame retardancy of epoxy resins containing intumescent flame retardant. *J Therm Anal Calorim.* 2009;95:605–8.
- Ribeiro SPS, Estevão LRM, Nascimento RSV. Brazilian clays as synergistic agents in an ethylenic polymer matrix containing an intumescent formulation. *J Therm Anal Calorim.* 2007;87:661–5.
- Han ZD, Fina A, Malucelli G. Thermal shielding performances of nano-structured intumescent coatings containing organo-modified layered double hydroxides. *Prog Org Coat.* 2015;78:504–10.
- Zheng ZH, Sun HM, Li WJ, Zhong SL, Yan JT, Cui XJ, Wang HY. Co-microencapsulation of ammonium polyphosphate and aluminum hydroxide in halogen-free and intumescent flame retarding polypropylene. *Polym Compos.* 2014;35:715–29.
- Zheng ZH, Yan JT, Sun HM, Cheng ZQ, Li WJ, Wang HY, Cui XY. Preparation and characterization of microencapsulated ammonium polyphosphate and its synergistic flame-retarded polyurethane rigid foams with expandable graphite. *Polym Int.* 2014;63:84–92.
- Wu K, Song L, Wang ZZ, Hu Y. Preparation and characterization of double shell microencapsulated ammonium polyphosphate and its flame retardance in polypropylene. *J Polym Res.* 2009;16:283–94.
- Chen XL, Jiao CM, Zhang J. Microencapsulation of ammonium polyphosphate with hydroxyl silicone oil and its flame retardance in thermoplastic polyurethane. *J Therm Anal Calorim.* 2011;104:1037–43.
- Lei ZQ, Cao YM, Xie F. Study on surface modification and flame retardants properties of ammonium polyphosphate for polypropylene. *J Appl Polym Sci.* 2012;124:781–8.
- Zheng ZH, Qiang LH, Yang T, Wang BN, Cui XJ, Wang HY. Preparation of microencapsulated ammonium polyphosphate with carbon source- and blowing agent-containing shell and its flame retardance in polypropylene. *J Polym Res.* 2014;21:443–57.

26. Jiang WZ, Hao JW, Han ZD. Study on the thermal degradation of mixtures of ammonium polyphosphate and a novel caged bicyclic phosphate and their flame retardant effect in polypropylene. *Polym Degrad Stabil.* 2012;97:632–7.
27. Teoh MM, Liu SL, Chung TS. Effect of pyridazine structure on thin-film polymerization and phase behavior of thermotropic liquid crystalline copolyesters. *J Polym Sci B Polym Phys.* 2005;43:2230–42.
28. Li J, Ke CH, Xu L, Wang YZ. Synergistic effect between a hyperbranched charring agent and ammonium polyphosphate on the intumescent flame retardance of acrylonitrile-butadiene-styrene polymer. *Polym Degrad Stabil.* 2012;97:1107–13.
29. Mahapatra SS, Karak N. *s*-Triazine containing flame retardant hyperbranched polyamines: synthesis, characterization and properties evaluation. *Polym Degrad Stabil.* 2007;92:947–55.
30. Huang GB, Liang HD, Wang Y, Wang X, Gao JR, Fei ZD. Combination effect of melamine polyphosphate and graphene on flame retardant properties of poly(vinyl alcohol). *Mater Chem Phys.* 2012;132:520–8.
31. Wang X, Li Y, Liao W, Gu J, Li D. A new intumescent flame-retardant: preparation, surface modification, and its application in polypropylene. *Polym Adv Technol.* 2008;19:1055–61.
32. Wang ZY, Han EH, Ke W. Influence of nano-LDHs on char formation and fire-resistant properties of flame-retardant coating. *Prog Org Coat.* 2005;53:29–37.
33. Qu BJ, Xie RC. Intumescent char structures and flame-retardant mechanism of expandable graphite-based halogen-free flame-retardant linear low density polyethylene blends. *Polym Int.* 2003;52:1415–22.